

# Source function extracted from single-event HBT correlation functions of hydrodynamical sources<sup>\*</sup>

HU Ying(胡颖)<sup>1</sup> FENG Ke-Xin(冯可心)<sup>1</sup> ZHANG Wei-Ning(张卫宁)<sup>1,2,1)</sup>

<sup>1</sup> School of Physics and Optoelectronic Technology, Dalian University of Technology, Dalian 116024, China

<sup>2</sup> Department of Physics, Harbin Institute of Technology, Harbin 150006, China

**Abstract:** We investigate the single-event two-pion correlation functions for the hydrodynamic particle-emitting sources with the fluctuating initial conditions generated by the Heavy Ion Jet Interaction Generator (HIJING). Using a three-dimension fast Fourier transform (FFT), we further extract the source functions from the single-event correlation functions. It is found that the inhomogeneity of the hydrodynamic sources with the fluctuating initial conditions lead to event-by-event fluctuations of the correlation functions and source functions.

**Key words:** single-event two-pion correlation function, source function, fast Fourier transform, hydrodynamic source, fluctuating initial condition

**PACS:** 25.75.-q, 25.75.Gz, 25.75.Nq **DOI:** 10.1088/1674-1137/38/4/044102

## 1 Introduction

In the heavy ion collisions at the highest energy of the Relativistic Heavy Ion Collider (RHIC) and at Large Hadron Collider (LHC) energies, the initial local-equilibrium systems are not spatially uniform and there are event-by-event fluctuations of the initial quantities [1]. These fluctuating initial conditions (FIC) may affect the system evolution of space-time and lead to some changes of the final particle observables [1, 2]. Consequently, it is important to study the effect of the FIC in relativistic heavy ion collisions.

Hanbury-Brown-Twiss (HBT) interferometry is a useful tool for detecting the space-time structure of the particle-emitting sources produced in high energy heavy ion collisions [3–6]. Because of the limitation of data statistics, the usual HBT analyses in experiments are performed for mixed events. In these mixed-event analyses, some event-by-event fluctuations associated with the FIC are smoothed out [7, 8].

In order to investigate the influence of FIC on the source space-time structure, we examine the single-event HBT momentum correlation functions for the hydrodynamical sources with the FIC generated by the Heavy Ion Jet Interaction Generator (HIJING) [9]. We find that the space-time distributions of the sources with the FIC of HIJING are inhomogeneous. This inhomogeneity leads to large fluctuations of the single-event momentum correlation functions  $C(\mathbf{q})$ . Using a three-dimension fast

Fourier transform (FFT) we extract the source functions of the relative separation of two source points,  $S(\mathbf{r})$ , from the single-event correlation functions  $C(\mathbf{q})$ . The results indicate that the source functions exhibit event-by-event fluctuations for the inhomogeneous sources. In heavy ion collisions at LHC energies, the event multiplicity of identical pions may reach to about several thousands. Correspondingly, the number of correlated pion pairs in one event is about  $10^6$ . In this case, it is to be hoped that interferometry analysis for single events will be performed. Further development of the single-event HBT technique and attempts to observe the source inhomogeneity in space-time directly from the source functions  $S(\mathbf{r})$  will be of great interest.

## 2 Hydrodynamic evolution of the system with FIC

Because of the collision transparency, the systems formed in the heavy ion collisions at the RHIC highest energy and LHC energies are nearly baryon free. The ideal hydrodynamic description for the baryon free system is defined by local conservations of energy and momentum [10, 11],

$$\partial_\mu T^{\mu\nu} = 0, \quad (1)$$

where  $T^{\mu\nu} = (\epsilon + p)u^\mu u^\nu - pg^{\mu\nu}$  is the energy-momentum tensor for an ideal fluid,  $\epsilon$  and  $p$  are the energy density and pressure in the local rest frame of a fluid element which is moving with velocity  $\mathbf{v}$ ,  $u^\mu = \gamma(1, \mathbf{v})$  is the four-

Received 4 June 2013, Revised 14 July 2013

\* Supported by National Natural Science Foundation of China (11075027, 11275037)

1) E-mail: wnzhang@dlut.edu.cn

©2014 Chinese Physical Society and the Institute of High Energy Physics of the Chinese Academy of Sciences and the Institute of Modern Physics of the Chinese Academy of Sciences and IOP Publishing Ltd

velocity,  $\gamma = (1 - \mathbf{v}^2)^{-1/2}$ , and  $g^{\mu\nu} = \text{diag}(+, -, -, -)$  is Minkowski metric tensor.

Under the assumption of Bjorken longitudinal boost invariance for ultrarelativistic heavy ion collisions [12], the hydrodynamics in (3+1) dimension may reduce to a (2+1) dimension hydrodynamics, and we need only to solve the transverse (in  $xy$ -plane) equations of motion [14],

$$\begin{aligned} \partial_t E + \partial_x[(E+p)v^x] + \partial_y[(E+p)v^y] &= -F(E, p, t), \\ \partial_t M^x + \partial_x(M^x v^x + p) + \partial_y(M^x v^y) &= -G(M^x, t), \\ \partial_t M^y + \partial_x(M^y v^x + p) + \partial_y(M^y v^y + p) &= -G(M^y, t), \end{aligned} \quad (2)$$

where  $F(E, p, t) = (E+p)/t$ ,  $G(M, t) = M/t$ ,  $E = T^{00}$  and  $M^i = T^{0i}$  ( $i = x, y$ ).

Assuming that the initial local equilibrium system is formed at time  $\tau_0$ , we construct the initial energy density at  $z=0$ , by using the AMPT code [13] in which the HIJING is used for generating the initial conditions, for the hydrodynamic evolving source with [14, 15]

$$\begin{aligned} \varepsilon(\tau_0, x, y; z=0) &= K \sum_{\alpha} \frac{p_{\perp\alpha}}{\tau_0} \frac{1}{2\pi\sigma_{\perp}^2} \\ &\times \exp\left\{-\frac{[x-x_{\alpha}(\tau_0)]^2 + [y-y_{\alpha}(\tau_0)]^2}{2\pi\sigma_{\perp}^2}\right\}. \end{aligned} \quad (3)$$

Here,  $p_{\perp\alpha}$  is the transverse momentum of parton  $\alpha$ ,  $x_{\alpha}(\tau_0)$  and  $y_{\alpha}(\tau_0)$  are the transverse coordinates of the parton at  $\tau_0$ ,  $\sigma_{\perp}$  is a transverse width parameter, and  $K$  is a scale factor that can be adjusted to fit the experimental data of produced hadrons.

In Fig. 1 we show the transverse distributions of energy density of the four single events for Pb+Pb collisions at  $\sqrt{s_{NN}}=2.76$  TeV, constructed with the HIJING for the impact parameter  $b=4$  fm and  $\tau_0=0.4$  fm/c. The unit of energy density is GeV/fm<sup>3</sup>. The parameters  $\sigma_{\perp}$  and  $K$  are taken to be 0.5 fm and 0.2. One can see that the transverse distributions of the initial energy density have large event-by-event fluctuations.

When solving the hydrodynamic equations of motion numerically, we also need an equation of state (EOS) to close the hydrodynamic Eq. (2). In the calculations, we use the parameterized EOS named s95p-PCE [16], which combines the hadron resonance gas at low temperature and the lattice QCD results at high temperature.

Figures 2(a1)–(a4) and (b1)–(b4) show the solutions of the transverse distributions of the energy density at  $z = 0$  and  $t = 3, 6, 9$  and  $12$  fm/c, for the single-event source with the HIJING initial conditions shown in Figs. 1(a) and (b), respectively. In the calculations,

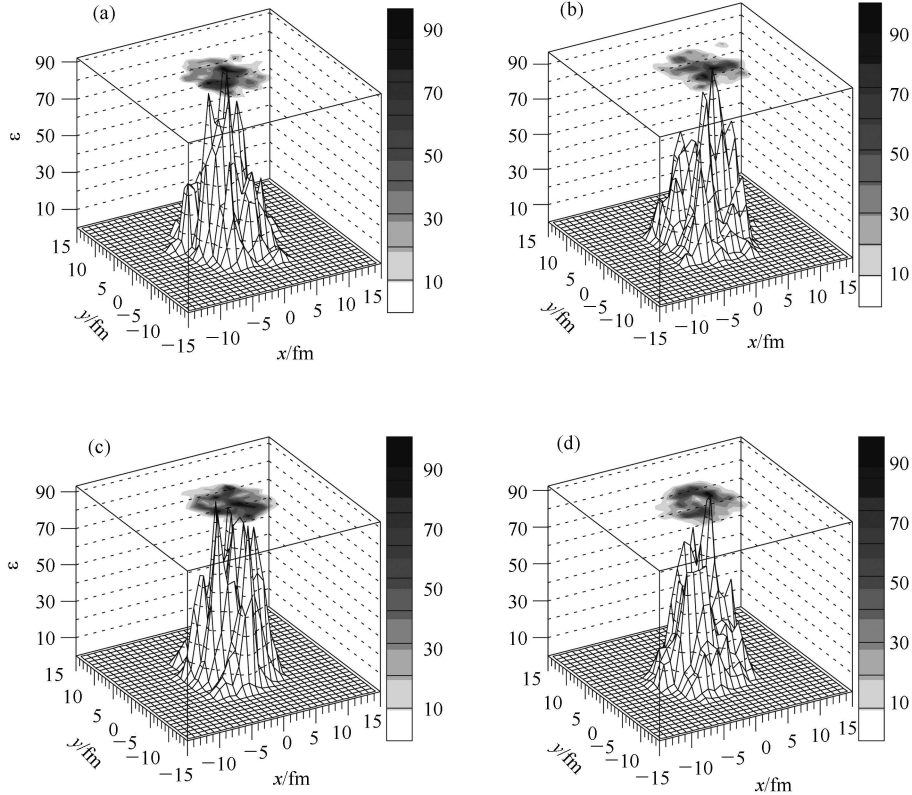


Fig. 1. The transverse distributions of initial energy density of the four single events for Pb+Pb collisions at  $\sqrt{s_{NN}}=2.76$  TeV, constructed with the HIJING for the impact parameter  $b=4$  fm and  $\tau_0=0.4$  fm/c. The unit of energy density is GeV/fm<sup>3</sup>.

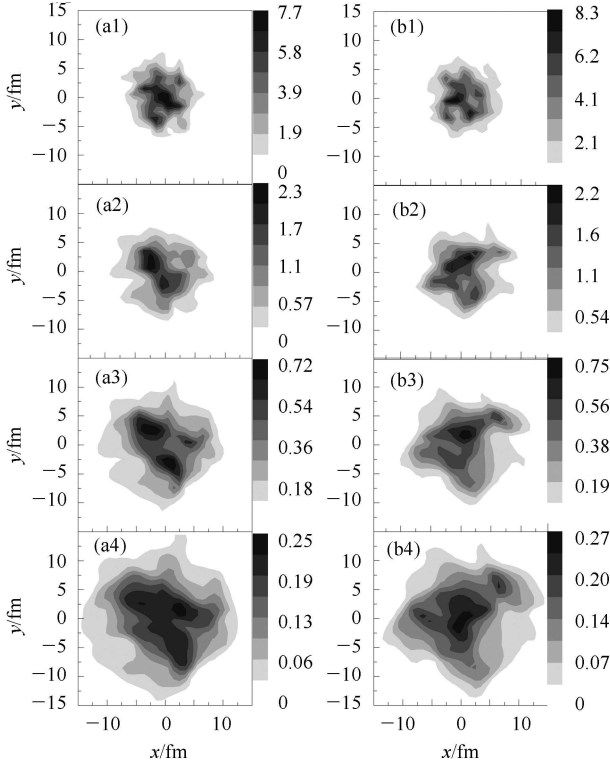


Fig. 2. The transverse distributions of energy density of the two single event at  $z=0$  and  $t=3$  fm/c [(a1) and (b1)],  $t=6$  fm/c [(a2) and (b2)],  $t=9$  fm/c [(a3) and (b3)], and  $t=12$  fm/c [(a4) and (b4)]. The initial conditions for panels (a1)–(a4) and (b1)–(b4) are those shown in Fig. 1(a) and (b), respectively. The unit of energy density is  $\text{GeV}/\text{fm}^3$ .

we use the relativistic HLLE scheme [10, 17, 18] and the Sod's operator splitting method [10, 18, 19] to solve the hydrodynamic equations in the transverse plane  $z=0$ , and obtain the hydrodynamic solutions at  $z \neq 0$  by the longitudinal boost invariance of Bjorken hypothesis [12, 14, 20]. The grid size in the HLLE calculations is taken to be  $\Delta x = \Delta y = 0.1$  fm, and the time step is taken to be  $\Delta t = 0.99\Delta x$ , which satisfies the Courant-Friedrichs-Lewy criterion,  $\Delta t/\Delta x < 1$  [10, 21]. From Fig. 2 it can be seen that the transverse distributions of the energy density have large fluctuations in space. These fluctuations survive even at the late stage of the evolution.

### 3 Single-event HBT correlation function and source function

The two-pion HBT correlation function is defined as the ratio of the two-pion momentum distribution

$P(\mathbf{p}_1, \mathbf{p}_2)$  to the production of single-pion momentum distribution  $P(\mathbf{p}_1)P(\mathbf{p}_2)$ ,

$$C(\mathbf{p}_1, \mathbf{p}_2) = \frac{P(\mathbf{p}_1, \mathbf{p}_2)}{P(\mathbf{p}_1)P(\mathbf{p}_2)}. \quad (4)$$

Assuming that the final pions are emitted at the space-time configuration characterized by a freeze-out temperature  $T_f$ , we can generate pion momentum  $\mathbf{p}_i$  ( $i=1,2$ ) according to Bose-Einstein distribution and obtain the two-pion and single-pion momentum distributions. In HBT interferometry, it is convenient to use the relative momentum  $\mathbf{q} = \mathbf{p}_1 - \mathbf{p}_2$  as a variable. The two-pion correlation function  $C(\mathbf{q})$  is constructed with the momentum distributions  $P(\mathbf{p}_1, \mathbf{p}_2)$  and  $P(\mathbf{p}_1)P(\mathbf{p}_2)$  by summing over  $\mathbf{p}_1$  and  $\mathbf{p}_2$  for the  $\mathbf{q}$  bins.

In Fig. 3(a)–(c) we show the two-pion correlation functions,  $C(q_x, q_y, |q_z| \leq 10 \text{ MeV}/c)$ , for the three single events with the HIJING initial conditions shown in Fig. 1(a)–(c). For comparison, we also show the correlation function for the mixed event with 80 single events in Fig. 3(d). In the calculations, the freeze-out temperature is taken to be 120 MeV and the number of correlated pion-pairs for each event is taken to be  $N_{\pi\pi} = 3 \times 10^6$ . One can see that the single-event correlation functions have prominent fluctuations that are related to the event-by-event fluctuations of the source space-time distributions (see Fig. 2).

In order to extract the information of source space-time distribution from the correlation functions, which are experimentally observable, we next examine the Fourier transform of the correlation functions. The Fourier transform of  $[C(\mathbf{q})-1]$  is

$$\begin{aligned} F(\mathbf{r}) &= \int \frac{d\mathbf{q}}{(2\pi)^3} e^{-i\mathbf{q}\cdot\mathbf{r}} [C(\mathbf{q})-1] \\ &= \int \frac{d\mathbf{q}}{(2\pi)^3} \{ \cos(\mathbf{q}\cdot\mathbf{r}) - i\sin(\mathbf{q}\cdot\mathbf{r}) \} [C(\mathbf{q})-1]. \end{aligned} \quad (5)$$

Because the correlation function  $C(\mathbf{q})$  is a real function greater than unity and possesses an inversion symmetry  $C(\mathbf{q}) = C(-\mathbf{q})$  [7], the imaginary part in Eq. (5) vanishes. By introducing the source function  $S(\mathbf{r})$  as the real part in Eq. (5), we have

$$S(\mathbf{r}) = \int \frac{d\mathbf{q}}{(2\pi)^3} \cos(\mathbf{q}\cdot\mathbf{r}) [C(\mathbf{q})-1]. \quad (6)$$

This presents the distribution of relative separation of the emission points for the two identical pions [7, 22, 23].

In this work, we use a three-dimensional FFT method [24] to calculate the source functions numerically. Expanding the cosine function in Eq. (6), we have

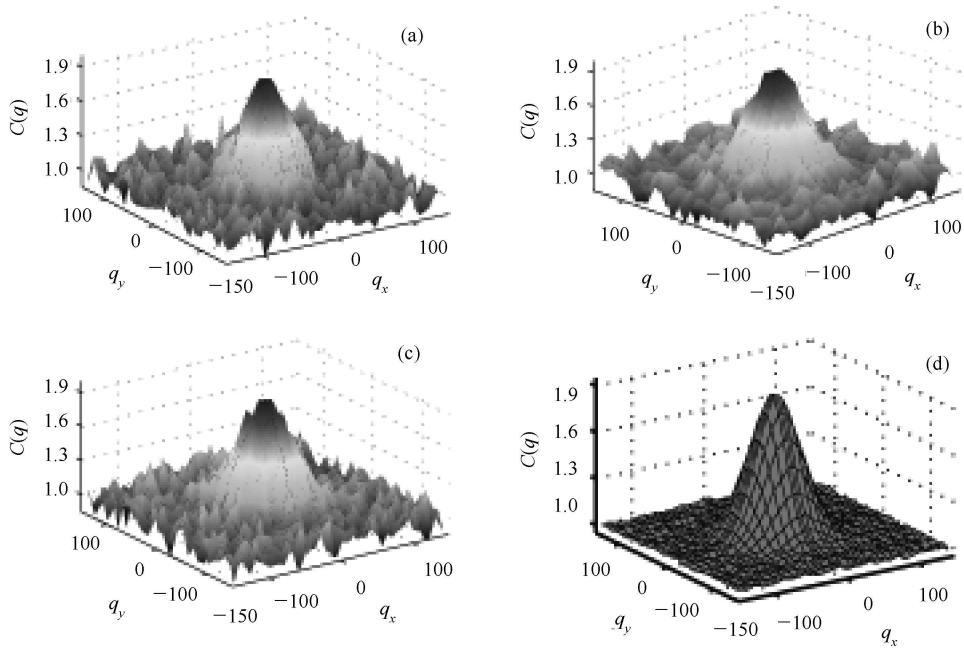


Fig. 3. Two-pion correlation functions  $C(q_x, q_y, q_z)$  of three single events (a)–(c) and the mixed event with 80 single events (d). Here the unit of relative momenta are MeV/c, and  $|q_z| \leq 10$  MeV/c.

$$\begin{aligned}
 S(\mathbf{r}) &= \int \frac{d\mathbf{q}}{(2\pi)^3} \cos(q_x x + q_y y + q_z z) R(\mathbf{q}) \\
 &= \int \frac{d\mathbf{q}}{(2\pi)^3} \left[ \cos(q_x x) \cos(q_y y) \cos(q_z z) \right. \\
 &\quad \left. - \cos(q_x x) \sin(q_y y) \sin(q_z z) - \sin(q_x x) \cos(q_y y) \right. \\
 &\quad \left. \times \sin(q_z z) - \sin(q_x x) \sin(q_y y) \cos(q_z z) \right] R(\mathbf{q}), \quad (7)
 \end{aligned}$$

where  $R(\mathbf{q}) = C(\mathbf{q}) - 1$ . Write Eq. (7) simply as

$$S(\mathbf{r}) = [A_1(\mathbf{r}) - A_2(\mathbf{r}) - A_3(\mathbf{r}) - A_4(\mathbf{r})] / (2\pi)^3, \quad (8)$$

where  $A_i(\mathbf{r}) / (2\pi)^3$  ( $i = 1, 2, 3, 4$ ) is the  $i$ th term in Eq. (7). The Fourier integral of the sine and cosine functions in Eq. (7) can be written as the standard form of the FFT package of DFFTPACK [24], in which the integrations go from zero to infinity, by the proper symmetric or antisymmetric reflectional relations. For example,

$$A_1(\mathbf{r}) = \int_0^\infty dq_z \cos(q_z z) [F_1(x, y, q_z) + F_1(x, y, -q_z)], \quad (9)$$

$$A_2(\mathbf{r}) = \int_0^\infty dq_z \sin(q_z z) [F_2(x, y, q_z) - F_2(x, y, -q_z)], \quad (10)$$

where

$$F_1(x, y, q_z) = \int_0^\infty dq_y \cos(q_y y) [E_1(x, q_y, q_z) + E_1(x, -q_y, q_z)],$$

$$F_2(x, y, q_z) = \int_0^\infty dq_y \sin(q_y y) [E_2(x, q_y, q_z) - E_2(x, -q_y, q_z)],$$

and

$$\begin{aligned}
 E_1(x, q_y, q_z) = E_2(x, q_y, q_z) &= \int_0^\infty dq_x \cos(q_x x) [R(q_x, q_y, q_z) \\
 &\quad + R(-q_x, q_y, q_z)].
 \end{aligned}$$

Also,  $A_3(\mathbf{r})$  and  $A_4(\mathbf{r})$  can be written as the standard form of the FFT package in a similar way.

With the above relations, we can obtain the source functions from two-pion correlation functions by using the FFT packages [24]. In Figs. 4(a), (b) and (c) we show the results of the source functions  $S(\mathbf{r})$  at  $z = 0, 4.13,$  and  $8.26$  fm, obtained by the FFT for the single-event two-pion correlation function presented in Fig. 3(a). The source function has a maximum at  $\mathbf{r} = 0$ . The region of its distribution is consistent with the source geometry.

From Fig. 4 it can be seen that the source functions obtained from single event are fluctuated. Since the correlation functions for the sources with FIC are fluctuated event-by-event, the fluctuations in the source functions should also be different event-by-event. In Fig. 5, (a), (b) and (c) we show the source functions  $S(x; y=0; z)$  versus  $x$  at  $z = 0, 4.13,$  and  $8.26$  fm, respectively. Here, the dashed lines are the results of the source functions extracted from the single-event two-pion correlation functions, as shown in Fig. 3(a)–(c), and the solid lines are the mixed event correlation functions in Fig. 3(d). One can see that there are large fluctuations in the source

functions of single events as compared to that of the mixed event. The fluctuating structures of the single-event source functions are different event-by-event. This event-by-event fluctuating structure of the relative separation of source points provides another more intuitive signature for the spatial inhomogeneity of the particle-emitting sources.

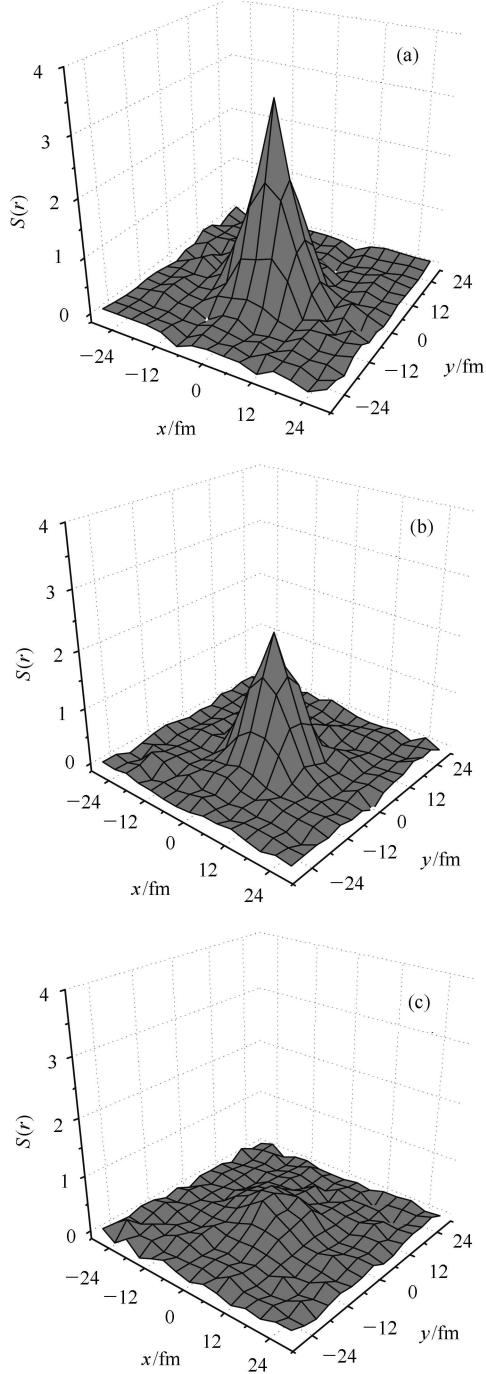


Fig. 4. The source function  $S(x, y, z)$  at (a)  $z=0$ , (b)  $z=4.13$  fm, and (c)  $z=8.26$  fm, obtained from single event. The unit of  $S(\mathbf{r})$  is  $[10^{-4} \cdot \text{fm}^{-3}]$ .

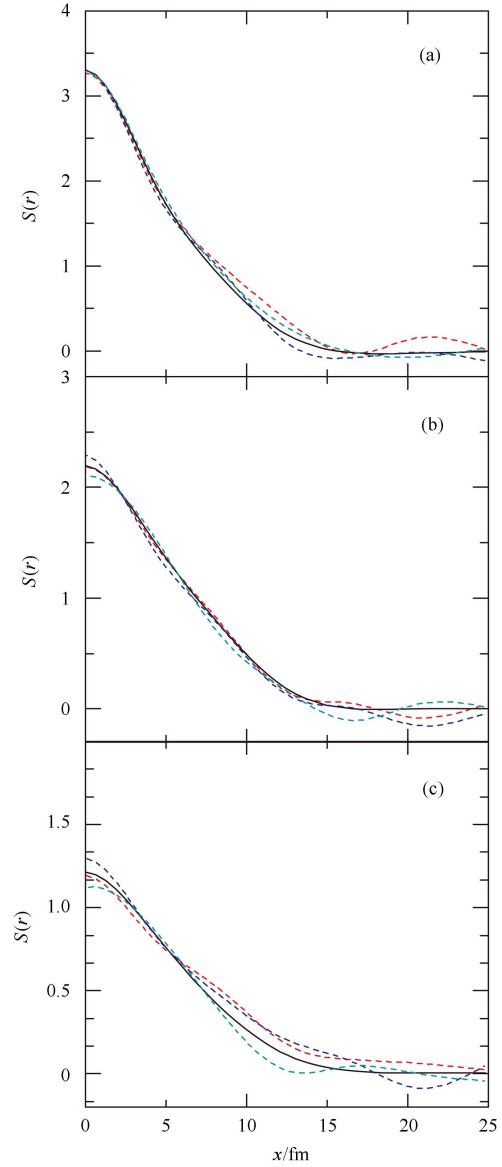


Fig. 5. The source functions  $S(x, y=0, z)$  versus  $x$  at (a)  $z=0$ , (b)  $z=4.13$  fm, and (c)  $z=8.26$  fm, respectively. The dashed lines are the results obtained from the three single-event correlation functions presented in Fig. 3(a)–(c). The solid lines are for that of the mixed event shown in Fig. 3(d). The unit of  $S(\mathbf{r})$  is  $[10^{-4} \cdot \text{fm}^{-3}]$ .

## 4 Summary and discussion

On an event-by-event basis, the density distributions of the particle-emitting sources produced in relativistic heavy ion collisions are inhomogeneous in space because of the fluctuations of the initial matter distribution in the collisions. In this work, we have examined the single-event two-pion HBT correlation functions for the hydrodynamical sources with the FIC generated by

HIJING. The results indicate that the source inhomogeneity associate with the FIC may lead to large fluctuations of the single-event HBT correlation functions. By performing a three-dimension FFT to the single-event HBT correlation functions, we extract the source functions  $S(\mathbf{r})$  of the inhomogeneous sources. We find that the source functions exhibit large spatial fluctuations and that they are different event-by-event. These event-by-event fluctuations of the spatial source functions provide a more intuitional signature of the inhomogeneous particle-emitting sources in relativistic heavy ion collisions.

In usual HBT analyses, the two-pion correlation functions are obtained with mixed-event samples because of

the limitation of data statistics. In this case, the event-by-event fluctuations of the correlation functions  $C(\mathbf{q})$  are washed out. With the smoothed momentum correlation functions, people can further obtain the source HBT radii by parameterized fits and extract the spatial source functions  $S(\mathbf{r})$  by the imaging technique [25–27]. As compared to the imaging technique, the FFT method is more suitable for the correlation functions with large fluctuations. As the collision energy increases, few- or single-event HBT analysis will be hoped for in high energy heavy ion collisions. It will be of great interest to develop few- and single-event HBT techniques, and to observe and understand the event-by-event source fluctuations.

## References

- 1 Adare A, Luzum M, Petersen H. arXiv:1212.5388 [nucl-th]
- 2 ZHANG W N, REN Y Y, Wong C Y. Phys. Rev. C, 2006, **74**: 024908; YANG Z T, ZHANG W N, HUO L et al. J Phys G, 2009, **36**: 015113; ZHANG W N, YIN H J, REN Y Y. Chin. Phys. Lett., 2011, **28**: 122501
- 3 Wong C Y. Introduction to High-Energy Heavy-Ion Collisions. Singapore: World Scientific, 1994. Chap 17
- 4 Wiedemann U A, Heinz U. Phys. Rept, 1999, **319**: 145–230
- 5 Weiner R M. Phys. Rept, 2000, **327**: 249–346
- 6 Lisa M A, Pratt S, Soltz R, Eiedemann U. Ann. Rev. Nucl. Part. Sci., 2005, **55**: 357–402
- 7 Wong C Y, ZHANG W N. Phys. Rev. C, 2004, **70**: 064904
- 8 ZHANG W N, LI S X, Wong C Y et al. Phys. Rev. C, 2005, **71**: 064908; REN Y Y, ZHANG W N, LIU J L. Phys. Lett. B, 2008, **669**: 317–320
- 9 WANG X N. Phys. Rept. 1997, **280**: 287–371
- 10 Rischke D H. arXiv:nucl-th/9809044
- 11 Kolb P F, Heinz U. arXiv:nucl-th/0305084
- 12 Bjorken J D. Phys. Rev. D, 1983, **27**: 140–151
- 13 LIN Z W, Ko C M, LI B A, ZHANG B, Pal S. Phys. Rev. C, 2005, **72**: 064901
- 14 Gyulassy M, Rischke D H, ZHANG B. Nucl. Phys. A, 1997, **613**: 397–434
- 15 PANG L G, WANG Q, WANG X N. Phys. Rev. C, 2012, **86**: 024911
- 16 Chun S, Heinz U, Huovinen P, Song H C. Phys. Rev. C, 2010, **82**: 054904
- 17 Schneider V, Katscher U, Rischke D H et al. J. Comput. Phys., 1993, **105**: 92–107
- 18 Rischke D H, Bernard S, Maruhn J A. Nucl. Phys. A, 1995, **595**: 346–382; Rischke D H, Gyulassy. Nucl. Phys. A, 1996, **608**: 479–512
- 19 Sod G A. J. Fluid. Mech., 1977, **83**: 785
- 20 Baym G, Friman B L, Blazot J P et al. Nucl. Phys. A, 1983, **407**: 397–434
- 21 Courant R, Friedrichs K O, Lewy H. Math. Ann., 1928, **100**: 32–74
- 22 Koonin S E. Phys. Lett. B, 1977, **70**: 43
- 23 Pratt S, Csörgö, Zimányi T. Phys. Rev. C, 1990, **42**: 2646
- 24 Pumphrey H C, Swarztrauber P N. DFFTPACK package. available from the fftpack site at www.netlib.org
- 25 Brown D A, Danielewicz P. Phys. Rev. C, 1998, **57**: 2474–2483; Brown D A, Danielewicz P. Phys. Rev. C, 2001, **64**: 014902
- 26 Danielewicz P, Pratt S. Phys. Rev. C, 2007, **75**: 034907
- 27 ZHANG W N, YANG Z T, REN Y Y. Phys. Rev. C, 2009, **80**: 044906